Ali MOSALLANEJAD[1], Abbas SHOULAIE[2]

Iran University of Science and Technology, Tehran, Iran (1)& (2)

Calculation of Coil Inductance in Tubular Linear Reluctance Motor using Three Dimensional FEM

Abstract. This paper reports a study of coil inductance in every plunger positions in tubular linear reluctance motors (TLRMs) with open type magnetic circuits. In this paper, all inductance (minimum and maximum inductance) calculation methods in winding of tubular linear reluctance motors are described. Furthermore, a new approach in maximum inductance calculation based on energy method is proposed. Electromagnetic finite-element analysis is used for motor simulation and coil inductance calculation. Moreover, inductance of a prototype TLRM was measured with experimental methods. Simulation results of coil inductance calculation using 3-D FEM with coil current excitation is compared to theoretical and experimental results. The comparison yields a good agreement.

*Streszczenie. Przedstawiono analizę indukcyjności cewki stosowanej w rurowym reluktancyjnym silniku liniowym z otwartym obwodem magnetycznym. Zastosowano metodę elementu skończonego do symulacji silnika i obliczania indukcyjności cewki. (**Obliczenia indukcyjności cewki w rurowym liniowym silniku reluktancyjnym**)*

Keywords: Tubular linear reluctance motors, minimum and maximum inductance, FEM analyses
Słowa kluczowe: silnik reluktancyjny, indukcyjność, metoda element skończonego

Introduction

Using electric circuit theory, linear motors under both ac and dc supplies have been greatly studied [1– 5]. It must be mentioned here that linear dc motors have lower efficiency than ac ones. However, they are widely used in lots of applications [6]. Linear motors have several types which differ in construction. TLRM is a linear motor that can operate in different modes of operation such as self-oscillating, switched-oscillating and accelerator.

A TLRM consists of two major parts i.e. a moving part, also known as plunger, and a stator. Stator is a winding which is fed by a dc source and produces the magnetic field. A TLRM in its simplest form is illustrated in Fig. 1 [6],[7].
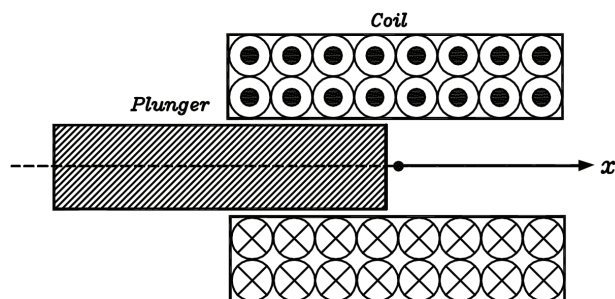

Fig 1. Tubular linear reluctance motor with open magnetic circuit

A TLRM is a linear motor which its operation is based on the tendency of its movable part to move to a position with higher inductance or, in other words, lower reluctance. This is exactly how force and velocity is produced in this motor.

As the plunger moves into the coil, its ferromagnetic material reduces the reluctance and therefore magnetic force is developed due to the change in motor reluctance. The ferromagnetic plunger has a greater magnetic permeability than the air it replaces. As a consequence, the magnetic flux can be formed more easily when the plunger is placed in the center of the coil. At this point, the reluctance is at its minimum for a given flux level; it is also the position of the least energy. When displaced from the centered position, magnetic forces will always act to restore the plunger to its previous position. TLRM is consisted of a series of coils activated sequentially to pull the plunger along the coil. Note that the plunger is only pulled, and is never pushed. This is a disadvantage of TLRMs when compared to other synchronous accelerators that can push

and pull by choosing the relative polarity of the armature and stator windings.

TLRMs have been investigated in various types of magnetic circuits with analyzing magnetic field, calculating integral parameters of the field and determining static characteristics of the motor in [6]. Moreover the performance of the motor under both ac and dc supplies is studied in [7].

Design rules of a reluctance accelerator are described in [8]; this paper also discusses the accelerator control methods and their predicted performances. TLRM different modes of operation are discussed completely in [9]. This paper also discusses the design and modeling of TLRM in self-oscillating mode. Equivalent circuit parameters of TLRM are obtained using experimental method in [10]. Also in [11], a permanent magnet linear oscillating accelerator is analyzed theoretically and validated via experimental results. The coupled field-circuit model of the three-stage reluctance accelerator is presented in [12]. Another work has studied the design features of variable-air gap, cylindrical and variable reluctance actuators [13].

Many other researches that have been investigating TLRMs behavior, mostly focused on evaluation of TLRM's operation modes and structure. While, to our knowledge, no research has concentrated on calculating minimum and maximum inductance, and, in all the mentioned references, the minimum and maximum inductance is obtained by measurement method. Even it is mentioned in [14] that" The dynamic inductance of the motors was not calculated on the basis of the magnetic field analysis. They often were obtained with using measured inductance only".

In this paper, all methods of minimum inductance calculation are described and a new approach in maximum inductance calculation is proposed based on energy method. In the proposed method, it is necessary to calculate the field intensity inside the iron core. Therefore, in this paper, field intensity inside the iron core is achieved with regard to eddy current. Finite element method is used for motor simulation and its inductance calculation in every plunger position. For evaluating simulation and calculation results, a prototype TLRM was built and its inductance was measured. Finally, calculation, simulation, and experimental results of coil inductance are compared.

Methods of the inductance calculation

In the following sections, all the methods used for TLRMs windings inductance calculation are described. Coil

inductance calculation must be performed for two main plunger positions i.e. when the plunger is completely outside the coil, and when the plunger is fully inside the coil. The two mentioned positions yield to the minimum and maximum inductances, respectively. In the first subsection, several methods for calculating the minimum inductance is presented, and in the second subsection the proposed method for calculating maximum inductance is explained.

A. Minimum inductance calculation

Operation of the tubular linear reluctance motor depends strongly on the motor inductance profile. Therefore, calculating the motor inductance with a good accuracy is very important. The motor inductance is proportional to different factors such as, coil and plunger dimensions, excitation currents, and plunger position. The winding inductance, L, is determined according to the plunger position. Since the coil inductance is dependent on the plunger position, the inductance profile is estimated as follows:

$$(1) \qquad L = L_m \left[1 + \cos\left(\frac{\pi}{l} x \right) \right] + L_{min}$$

$$(2) \qquad L_m = \frac{L_{max} - L_{min}}{2}$$

where: L_{min} : Coil inductance when the plunger is out of the coil, L_{max} : Coil inductance when the plunger is completely inside the coil, so that (x= 0).

The coil minimum inductance is approximately equal to air core reactor inductance. In the following, all methods of minimum inductance calculation are presented. In general, the coil inductance L is determined from the magnetic flux linkage λ as:

$$(3) \qquad L = \frac{\lambda}{i} = \frac{N\varphi}{i}$$

$$(4) \qquad \varphi = \Lambda_m N i$$

Where: N is the number of coil turns, Λ_m is the permeance of the main flux .

$$(5) \qquad \Lambda_m = \mu_0 \mu_r \frac{A}{l}$$

Substituting (5) into (4) and (4) into (3) yields:

$$(6) \qquad L = \mu_0 \mu_r \frac{N^2 A}{l}$$

Equation (6) is the main formula for inductance calculation, but using (6) for calculating TLRMs minimum inductance is not accurate enough. Therefore, other methods with more satisfactory results should be extracted.

One of the most common models in the electromagnetic analysis of electrical motors and electromagnetic devices are current filament models. In this paper the current filament methodology is used to calculate coil minimum inductance in TLRM.

The axisymmetric configuration of the coil allows the subdivision of the coil into coaxial rings, in which a uniform current density is assumed.

Since the assumed rings are coaxial, the following formula is used for determining the mutual inductance between i^{th} and j^{th} rings [15]:

$$(7) \qquad L_{ij} = 2\mu_0 \sqrt{\frac{r_i r_j}{m}} \left[\left(1 - \frac{m}{2} \right) K(m) - E(m) \right]$$

where: r_i : radius of the ith ring, r_j : radius of the jth ring, d_{ij} : axial distance between ith and jth rings and m is obtained from:

$$(8) \qquad m = \frac{4 r_i r_j}{\left(r_i + r_j \right)^2 + d_{ij}^2}$$

$K(m)$ and $E(m)$ represent the first and second type of elliptical integrals, respectively. The self inductance of the ith ring is obtained from [16]:

$$(9) \qquad L_i(r_i , h_i) = \mu_0 r_i \left(Ln \frac{8 r_i}{h_i} - 0.5 \right)$$

where h_i is the diameter of the ith ring conductor of the motor coil. The self inductance of the coil is given by:

$$(10) \qquad L_{n+1,n+1} = \sum_{1}^{n} \left(L_i + \sum_{\substack{i=1 \\ i \neq j}}^{n} L_{ij} \right)$$

In the above equation, L_{ij} and L_i are presented in (7) and (9), respectively.

Another Method for calculating coil minimum inductance in TLRM is explained in the following. A simplified form of an open magnetic type of TLRM without plunger is shown in Fig. 2 [17].
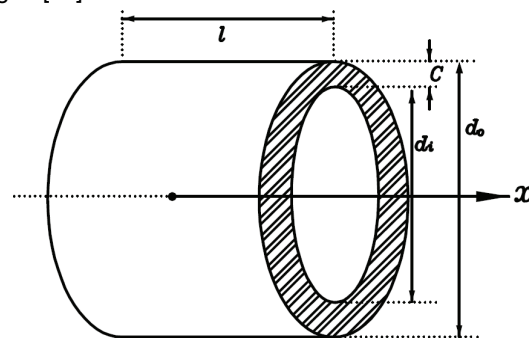

Fig. 2. Schematic showing the simplified coil geometry

The self inductance of the coil is given by:

$$(11) \qquad L = \phi d N^2 \quad (\mu H)$$

where,

$$(12) \qquad \phi = \frac{0.1 \pi^2}{0.45 + \alpha + \mu + \left[\frac{2}{3} \right] \alpha \rho \left[\frac{(\alpha+1)}{(\alpha+2)} \right]}$$

$$(13) \qquad \alpha = \frac{l}{d} \quad , \rho = \frac{c}{d}$$

$$(14) \qquad d = \frac{(d_0 + d_1)}{2}$$

In above equation: $l =$ length of coil, $c =$ thickness of coil, $d_i =$ coil inner diameter, $d_o =$ coil outer diameter.

Experimental results indicate that the minimum inductance calculated using (10) and (11) has a satisfactory accuracy. It should be mentioned that the response time of current filament method is increased if the number of coil turns is increased. As turn numbers of our TLRM was considerably high, equation (11) was used for calculating the minimum inductance.

An approximated formula for calculating minimum inductance has been presented by [18] as:

(15) $$L = 3.95 \frac{r^2 \times N^2}{l + 0.9r} \quad [\mu H]$$

Where N and l are the number of turns and length of coil, respectively. The square of the radius in the numerator arises from the area inside the circular windings over which flux is measure [18].

From [19, 20], the inductance for solenoid coils is:

(16) $$L = 1.6994 \times 10^{-6} \times r \times N^2 \quad [H]$$

Where r is the mean radius of the coil in meters and N is the number of turns.

B. Maximum Inductance Calculation

The coil inductance with the plunger placed in the centre of the coil, so that $x = 0$, is at its maximum. This situation is shown in Fig. 3.
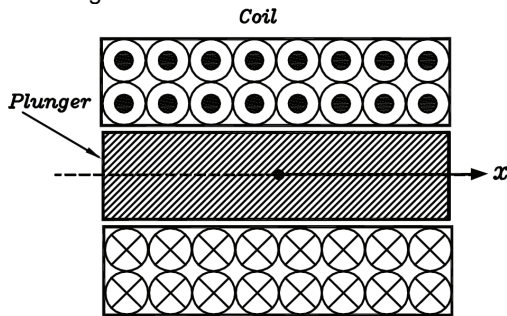

Fig. 3. Tubular linear reluctance motor with open magnetic system when the plunger placed in the centre of the coil

In this paper energy method is utilized in order to calculate the maximum inductance. The energy stored in an inductor is actually stored in its surrounding magnetic field. Hereby, an explicit formula for the stored energy in a magnetic field is obtained. The stored energy in the coil when the current I flows through the winding is as follows:

(17) $$W = \frac{1}{2} L I^2$$

where L is the self-inductance. Moreover, the stored energy in the solenoid can be rewritten as follows:

(18) $$W = \frac{B^2}{\mu_0} V$$

(19) $$B = \mu_0 \frac{NI}{l}$$

where V is the volume of the solenoid. The above equations are simply used when the plunger is out of the coil. If the plunger enters the coil, it is necessary to calculate the field intensity inside the iron core.

Usually in electrical motors the iron core is laminated, while in TLRMs, it is integrated. Therefore, a high eddy current is produced inside the core. Fig.4 shows a TLRM cylindrical core (plunger) without the coil.
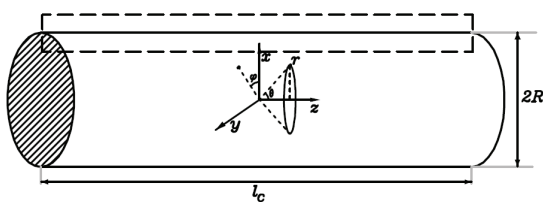

Fig.4. schematic of the iron core

In Fig.4, R is the core's radius and l_c is the length of the iron core. The current $i(t)$ in the winding flows in the φ direction of the cylindrical coordinate system shown in Fig. 4.

With flowing current in the coil, in one dimensional analysis, the flux line and the magnetic field intensity vector in the core has only the component along the z axis which depends only on the r coordinate along the core's radius and time, t, and the eddy current density vector has the φ-directed component $J_\varphi(r,t)$ only. The Ampere's circuital law is applied to a rectangular line consisting of a path located inside the iron core and the air gap (as indicated by the dashed line in Fig. 4). Therefore, we can write [21]:

(20) $$H_c(r,t)l_c + H_a(r,t)l_a = Ni(t) + l_c \int_r^R J_\theta(r,t)dr$$

where $H_c(r,t)$ and $H_a(r,t)$ are the magnetic field intensities in the iron core and in its related air gap, respectively. Also, l_a is the average length of flux path through the air gap.

Assuming $\phi_a = \phi_c$, we can write

(21) $$H_a = \mu_{rc} H_c \frac{A_c}{A_a}$$

In TLRMs, the flux path is consisted of two parts i.e. air gap and iron core. In (20), core length (l_c) is specified but the average length of flux path through the air gap should be determined. The following formula is proposed to calculate l_a:

(22) $$l_a = \frac{\mu_o N i(t)}{B_c} \cdot \frac{A_c}{A_a} - \frac{l_c}{\mu_{rc}} \cdot \frac{A_c}{A_a}$$

where μ_{rc} is the relative magnetic permeability of the iron core. Substituting (22) and (21) into (20) yields:

(23) $$\frac{\mu_c H_c(r,t).N.i}{B_c} = Ni(t) + l_c \int_r^R J_\theta(r,t)dr$$

In left side of (23), $N.i$ can be rewritten in the form follows:

(24) $$N.i(t) = H.l$$

and

(25) $$H = \mu_e.B_c$$

where μ_e is the equivalent magnetic permeability defined by [22]:

(26) $$\mu_e = \mu_o \frac{\mu_{rc}}{1 + n(\mu_{rc} - 1)}$$

where

(27) $$n \cong \frac{D_c^2}{l_c^2}(\ln \frac{2l_c}{D_c} - 1)$$

The above equation has a very high accuracy if the inner diameter of the winding is equal to the iron core diameter. Otherwise its accuracy will be decreased. In TLRMs, (26) is not usable since there is significant air gap between plunger and coil; therefore in this paper, equivalent magnetic permeability (μ_e) is measured by experimental results.

Substituting (25) and (24) into (23), equation (23) can be rewritten in the following form:

(28)
$$\frac{\mu_c H_c(r,t).l}{\mu_e} = N i(t) + l_c \int_r^R J_\theta(r,t) dr \quad , 0 < r < R$$

From (28), we can write

(29)
$$\frac{\partial H_c(r,t)}{\partial r} = \frac{l_c}{l} \cdot \frac{\mu_e}{\mu_c} \cdot \frac{\partial}{\partial r}\left[\int_r^R J_\theta(r,t) dr\right] = -\frac{l_c}{l} \cdot \frac{\mu_e}{\mu_c} J_\theta(r,t)$$

Faraday's law for the problem under consideration can be written as

(30)
$$\frac{\partial E_\varphi(r,t)}{\partial r} = -\frac{\partial B_c(r,t)}{\partial t}$$

Applying Ohm's law and using (29) and (30), we can write

(31)
$$\frac{\partial^2 H_c(r,t)}{\partial r^2} = \frac{l_c}{l} \cdot \frac{\mu_e}{\rho} \cdot \frac{\partial H_c(r,t)}{\partial r}$$

Equation (31) can be rewritten into the following equation for sinusoidal steady state conditions of an angular frequency ω.

(32)
$$\frac{\partial^2 \hat{H}_c(r)}{\partial r^2} = K^2 \cdot \frac{\partial H_c(r)}{\partial r}$$

where

(33)
$$K = \sqrt{\frac{j\omega \mu_e l_c}{\rho_c l}} = \sqrt{\frac{l_c}{l}} \frac{1+j}{\delta_t}$$

and

(34)
$$\delta_t = \sqrt{\frac{\rho_c}{\pi \mu_e f}}$$

The differential equation (32) has a general solution given by

(34)
$$\hat{H}_c = \hat{C} \cosh K r$$

Applying the boundary conditions to (34) yields

(35)
$$\hat{H}(r) = H_{BO} \frac{\cosh(K r)}{\cosh(K R)}$$

where H_{BO} is the magnetic field intensity phasor at the boundary of the core .

In order to calculate H_{BO} using the differential form of the Maxwell–Faraday law, first we should calculate eddy-current density phasor $\hat{J}_\theta(r)$ in the core as follows:

(36)
$$\hat{J}_\varphi(r) = (\nabla \times \hat{H}_c(r))_\varphi = -H_{BO}\sqrt{\frac{l_c}{l}} \frac{1+j}{\delta_t} \frac{\sinh(\sqrt{\frac{l_c}{l}}\frac{1+j}{\delta_t}r)}{\cosh(\sqrt{\frac{l_c}{l}}\frac{1+j}{\delta_t}R)}$$

Substituting (36) into (28), and solving (28), the following relation is achieved:

(37)
$$H_{BO} = \frac{\mu_e}{\mu_c} \frac{NI}{l}$$

As mentioned before, H_{BO} is the magnetic field intensity phasor at the boundary of the core and I is the phasor of the sinusoidal current flowing through the coil. Substituting (37) into (35), magnetic field intensity inside the iron core is calculated.

After determining field intensity inside the iron core, energy stored in the core can be calculated.

When the plunger enters the coil as long as the distance Δx, the stored energy is calculated from the following equation:

(38)
$$W_m(x_0 + \Delta x) = W_m(x_0) + \frac{1}{2}\frac{B_c^2}{\mu_e} S \Delta x$$

and

(39)
$$B_c = \mu_c . H_c$$

where $W_m(x_0)$ is the stored energy in the coil when the plunger is out of the coil. After substituting (37) into (39) and (39) into (38), the stored energy can be described as follows:

(40)
$$W_m(x_0 + \Delta x) = \frac{1}{2}L_{min}I^2 + \frac{1}{2}\mu_e\frac{N^2 I^2}{l^2} S \Delta x$$

When plunger enters the coil as long as the distance x, the stored energy is obtained by integrating equation (40) from $0 \rightarrow x$:

(41)
$$W_m(x_0 + \Delta x) = \frac{1}{2}L_{min}I^2 + \int_0^x \frac{1}{2}\mu_e\frac{N^2 I^2}{l^2} S \Delta x$$

Equation (41) can then be written in the following form

(42)
$$W_m(x_0 + \Delta x) = \frac{1}{2}L_{min}I^2 + \frac{1}{2}\mu_e\frac{N^2 I^2}{l^2} S x$$

In the above equation, the first term describes the coil energy when the plunger is out of the coil and the second term describes the energy stored in the plunger. When the center of the plunger is placed at the centre of the coil, the stored energy in the motor is calculated by substituting $x = l_c$ in (42).

(43)
$$W_m(x_0 + \Delta x) = \frac{1}{2}L_{min}I^2 + \frac{1}{2}\mu_e\frac{N^2 I^2}{l^2} S l_c$$

Equation (43) can be rewritten as:

(44)
$$\frac{1}{2}LI^2 = \frac{1}{2}L_{min}I^2 + \frac{1}{2}\mu_e\frac{N^2 I^2}{l^2} S l_c$$

As the center of the plunger is placed at the centre of the coil, the coil inductance is at its maximum. Consequently, (44) can be rewritten as:

(45)
$$\frac{1}{2}L_{max}I^2 = \frac{1}{2}I^2(L_{min} + \mu_e\frac{N^2}{l^2} S l_c)$$

According to Eq. (45), maximum inductance L_{max} is given by:

(46)
$$L_{max} = (L_{min} + \mu_e\frac{N^2}{l^2} S l_c)$$

Where: N is the coil turns, S is the cross section of plunger, l_c is the length of the plunger, I is the length winding, L_{min} is the coil minimum inductance that can be calculated form (10) or (11).

As TLRM coil inductance varies according to plunger position, it is necessary to calculate the coil inductance in every plunger position in order to obtain the dynamic model of TLRM.

The most important characteristic of (46) is that it can calculate the coil inductance in every plunger position. To obtain coil inductance in every position of the plunger, we

have to substitute the plunger length which is inside the coil with l_c.

Calculation of minimum and maximum inductance of laboratory model using FEM

The basic geometrical data of the prototype TLRM which was built in laboratory is given in Table 1.

Table 1.Motor parameters

Symbol	Quantity	Value
N	Number of turn	710
D_{ci}	Coil inner diameter(mm)	40
D_{co}	Coil outer diameter(mm)	52
D_{po}	Plunger outer diameter(mm)	35
l_c	Length of plunger(mm)	200
l_w	Length of winding(mm)	200
μ_{rc}	Relative magnetic permeability	380
r	resistance coil(Ω)	0.98
d	Conductor diameter(mm)	0.0016

Because of axial symmetry of the plunger, the three dimension FEM analysis is performed for a quarter of plunger area which is shown in Fig.5.
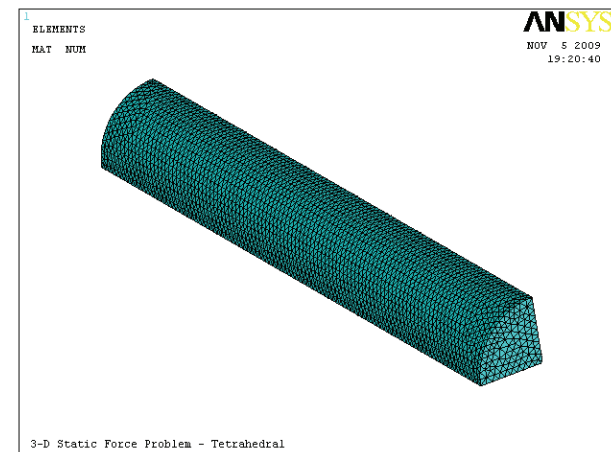

Fig.5. The plunger model used in three dimension FEM

In order to evaluate the proposed method, the prototype TLRM is modeled using 3-D FEM at a constant current during plunger movement. It must be noted that for this analysis, iron core nonlinear magnetic characteristic which was imported in the software, was obtained from several experiments performed on the iron core. When plunger enters the coil, the inductance increases and reaches its maximum while the plunger is completely inside the coil. Having the amount of inductance in every plunger position is essential for dynamic modeling. Therefore, motor inductance, when the plunger is moving through the coil, is measured with 3-D FEM. The results obtained from FEM analysis are compared with the experimental results and the ones obtained from the proposed method.

The magnetic field of tubular linear reluctance motor when the plunger is out of the coil is shown in Fig. 6.

Simulation results of 3-D FEM analysis indicates that the minimum inductance of TLRM is about 3.8mH. Moreover, another 3-D FEM analysis was performed for calculating TLRM maximum inductance which obtained the value of 53.1mH.

The minimum inductances, calculated from equation (10) and (11) for the prototype motor are approximately equal to 3.9mH and 4.0mH, respectively. Furthermore the

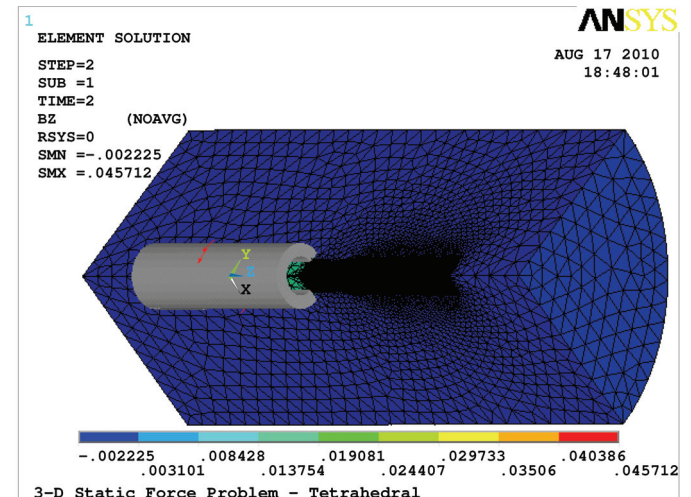maximum inductance, calculated from proposed method, is 51.1mH.

Fig. 6. the FEM schematic of coil and plunger

It should be mentioned that in (46) the value of equivalent magnetic permeability (μ_e) is calculated as follow:
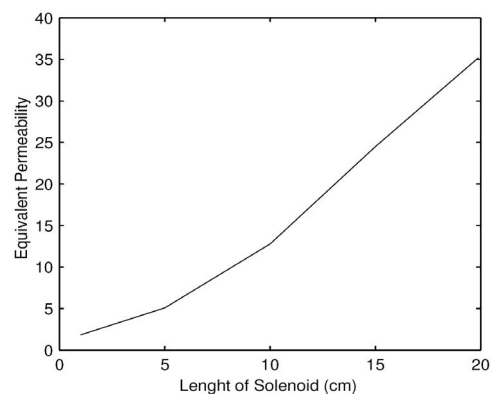
$$(47) \qquad \mu_e = \mu_o \mu_{re}$$

Fig.7. Experimental measured equivalent magnetic permeability according to position of plunger

In (47) μ_{re} is the value of related equivalent magnetic permeability that is achieved by the curve shown in Fig.7.

In Fig. 7, related equivalent magnetic permeability that was measured from experimental results is shown for all plunger positions. If the coil is without the plunger, equivalent magnetic permeability is equal to that of the air, but with the plunger entering the coil the equivalent magnetic permeability increases and reaches its maximum when the plunger is completely inside the coil. The maximum permeability is 35.7 according to Fig.7.

Experimental results

Another method to determine minimum and maximum inductance is to measure them through the experiment. In this method, AC voltage is applied to the motor and the motor current and voltage are measured. The mentioned experiment should be implemented for both minimum and maximum inductances. According to this method, minimum and maximum inductances are 3.95mH and 51.5mH, respectively.

In Table II, simulation results using FEM, computational and experimental results are presented.

Table 2. Simulation results using FEM, computational and experimental results

Methods	Min.Inductance (mH)	Max. Inductance (mH)
Eq. (10)	3.9	-
Eq (11)	4.0	-
Proposed Method	-	51.1
FEM	3.8	53.1
Experimental	3.95	51.5

As it is obvious in Table 2, the results of our proposed approach to calculate maximum inductance is close to simulation and experimental results which evaluates the proposed approach and proves its accuracy.

As mentioned earlier, in TLRM analysis, motor inductance in every plunger position is needed. Some research groups [4~10] have used (1) to estimate the inductance profile. This inductance profile is dependent on the minimum and maximum inductances of the coil. These references have used the measurement method to determine the maximum and the minimum inductance.

In this paper, however, we proposed a method which not only calculates the maximum inductance but also is able to calculate the inductance in any position of plunger. It must be mentioned that the value of minimum inductance in (46) was obtained from (11). Fig. 8 compares the results of the proposed method, FEM results, and the results estimated using (1).
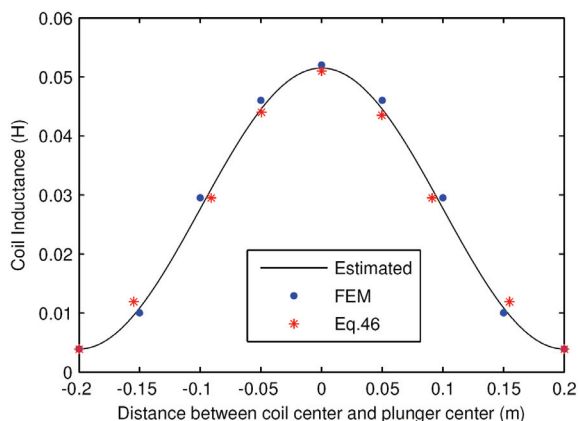

Fig. 8. Comparison of a simulation result with calculation wave form of coil inductance according to plunger position

Comparing the results of proposed method, FEM analysis, and the inductance profile achieved by (1) clearly shows the ability of the proposed method in calculating the coil inductance in any plunger position.

Conclusion

Operation of the tubular linear reluctance motor (TLRM) depends strongly on the motor inductance profile. Accuracy of coil inductance calculation in TLRM facilitates precise prediction of motor behavior. Experimental results indicate that the minimum inductance calculated using (10) and (11) have a high accuracy. It should be mentioned that response time of current filament method is increased if the number of coil turns is increased. The results of our proposed approach to calculate maximum inductance is close to simulation and experimental results which proves the proposed approach accuracy. The most important characteristic of the proposed method is its ability to calculate both the maximum inductance and the inductance

in any plunger position. μ_e is the most important parameter for calculating maximum inductance which was measured from experimental results. Since there is a considerable air gap between plunger and coil in TLRMs, equation (26) is not usable. Therefore, in this paper, equivalent magnetic permeability (μ_e) is measured by the experimental results.

REFERENCES
[1] Syed A. Nasar "Linear Electrical Motors : Theory , Design, and Practical Application ",Prentice- hall, 1987
[2] B. Marder, "A coilgun design primer," IEEE Trans. Magn., vol. 29, no. 1, pp. 701–705, Jan. 1993.
[3] E. R. Laithwaite, "A History of Linear Electric Motors" London, U.K.:Macmillan, 1987.
[4] J. J. Blakley, "A linear oscillating ferroresonant machine," IEEE Trans. Magn., vol. MAG-19, no. 4, pp. 1574–1579, Jul. 1983.
[5] S. A. Nasar and I. Boldea, " Linear Electric Motors". Englewood Cliffs, prentice-Hall, 1987.
[6] B. Tomczuk and M. Sobol, "Field analysis of the magnetic systems for tubular linear reluctance motors," IEEE Trans. Magn., vol. 41, no. 4, pp. 1300–1305, Apr. 2005
[7] E.A. Mendrela "Comparison of the Performance of a Linear Reluctance Oscillating Motor Operating Under AC Supply with One Under DC Supply" IEEE Transactions on Energy Conversion, Vol. 14, No. 3, September 1999
[8] D. A. Bresie and J. A. Andrews, "Design of a reluctance accelerator," IEEE Trans. Magn., vol. 27, no. 1, pp. 623–627, Jan. 1991.
[9] E.A. Mendrela Z.J. Pudlowski " Transients And Dynamics In A Linear Reluctance Self-Oscillating Motor" IEEE Trans. on Energy Conversion, vol. 7, No.1, March 1992
[10] J. Corda and shabbir M. Jamil, " Experimental Determination of Equivalent-Circuit Parameters of a Tubular Switched Reluctance Machine With Solid-Steel Magnetic Core" IEEE TRANS. on Industrial Electronics, vol. 57, No.1,Jan.2010
[11] Z.Q.Zhu, , X. Chen "Analysis of an E-Core Interior Permanent Magnet Linear Oscillating Actuator" IEEE Trans. on Magn. ,Vol. 45,No.10, Oct. 2009
[12] A. Waindok, G. Mazur, "A Mathematical and Physical Models of the Three-Stage Reluctance Accelerator" IEEE 2009
[13] S. Gibson G.W. Jewell R.E. Clark "Variable-air gap, cylindrical, linear variable reluctance actuators for high-force, medium-stroke applications" Published in IET Electric Power Applications, Revised on 21st January 2008
[14] Tomczuk and Sobol. " A Field-Network of a Linear Oscillating Motor and Its Dynamics Characteristics" IEEE Trans. on Magn., vol. 41, no. 8, August 2005
[15] L.L.Allgilberls, M.D.brown" Magnetocumulative Generators " Springer- verlag, pp.249-265.1999
[16] R.haghmaram, A.shoulaie, M.H. Khanzadeh" Parallel Connection of Traveling Wave Tubular Linear Induction Motors" Proc. 3th Int. Conf. on Technical and Physical problems in power Engineering, turkey. Pp. 192-199, 2006
[17] Thorborg , Kjeld " Power Electronic " Prentice Hall, 1988. 504 p.
[18] C. M. Fowler, R. S. Caird, W. B. Garn " An Introduction to Explosive Magnetic Flux Compression Generators " Los Alamos Report, LA-5890-MS,pp.1-7,1975
[19] L. Grover, "Inductance Calculations- Working Formulas and Tables". New York: Dover, 1962.
[20] D.K. Cheng , Fundamentals of Engineering Electromagnetic. Addison-Wesley, 1993.
[21] G. Grandi , Marian K.Kazimierczuk ,Antonio Massarini , Ugo Reggiani and Giuseppe Sancineto " Model of Laminated Iron – Core Inducted for High Frequencies" IEEE Trans. on Magn., vol. 40, no. 4, July 2004
[22] Slawomir Tumanski," Induction Coil Sensors – a review" journal of Measurement Science and Technology , vol. 18, January 2007

Authors: Ali Mosallanejad.(PHD Candidate), electrical department. Iran University of Science and Technology, Tehran, Iran
E-mail:mosallanejad@iust.ac.ir
prof. Abbas Shoulaie, electrical department. Iran University of Science and Technology, Tehran, Iran, E-mail: Shoulaie @iust.ac.ir